Title
Enhancement of acidic gases in biomass burning impacted air masses over Canada

Journal
Journal of Geophysical Research, 99(D1)

ISSN
0148-0227

Authors
Lefer, BL
Talbot, RW
Harriss, RH
et al.

Publication Date
1994-01-20

DOI
10.1029/93jd02091

JOURNAL OF GEOPHYSICAL RESEARCH, VOL. 99, NO. D1, PAGES 1721-1737, JANUARY 20, 1994

Enhancement of acidic gases in biomass burning impacted air masses over Canada

B. L. Lefer,[1] R. W. Talbot,[1] R. C. Harriss,[1] J. D. Bradshaw,[2] S. T. Sandholm,[2]
J. O. Olson,[2] G. W. Sachse,[3] J. Collins,[3] M. A. Shipham,[3] D. R. Blake,[4]
K. I. Klemm,[1,5] O. Klemm,[1,5] K. Gorzelska,[1,6] and J. Barrick[3]

Biomass-burning impacted air masses sampled over central and eastern Canada during the summer of 1990 as part of ABLE 3B contained enhanced mixing ratios of gaseous HNO_3, HCOOH, CH_3COOH, and what appears to be $(COOH)_2$. These aircraft-based samples were collected from a variety of fresh burning plumes and more aged haze layers from different source regions. Values of the enhancement factor, $\Delta X/\Delta CO$, where X represents an acidic gas, for combustion-impacted air masses sampled both near and farther away from the fires, were relatively uniform. However, comparison of carboxylic acid emission ratios measured in laboratory fires to field plume enhancement factors indicates significant in-plume production of HCOOH. Biomass-burning appears to be an important source of HNO_3, HCOOH, and CH_3COOH to the troposphere over subarctic Canada.

1. Introduction

In addition to the direct impact of degrading local air quality, emissions from biomass-burning may play a role in determining global atmospheric chemistry and climate [*Crutzen and Andreae*, 1990]. Biomass-burning also appears to be an important source of atmospheric acids such as nitric (HNO_3), formic (HCOOH), and acetic (CH_3COOH) acids [*LeBel et al.*, 1988; *Talbot et al.*, 1988b; *Keller et al.*, 1991; *Helas et al.*, 1992]. These atmospheric species are major acidity components of wet and dry deposition in remote regions [*Keene et al.*, 1983; *Talbot et al.*, 1990b; *Lacaux et al.*, 1991].

During the NASA Arctic Boundary Layer Expedition (ABLE) 3B to the Canadian subarctic (July-August 1990) the aircraft missions frequently encountered air masses impacted by biomass-burning emissions [*Harriss et al.*, this issue (a, b)]. Within these biomass-burning impacted air masses, we measured enhanced mixing ratios of gaseous HCOOH, CH_3COOH, HNO_3, and oxalic ($(COOH)_2$) acid. The first group of flights were staged out of North Bay, Ontario, (missions 2-9) and flown over subarctic wetlands of the Hudson Bay lowlands. In addition, two flights were based out of Churchill, Manitoba, to investigate the boundary layer and lower free troposphere over the subarctic tundra of northern Manitoba and Saskatchewan (missions 6 and 7). Mission 10 was a transit flight to Goose Bay, Newfoundland, where a second series of flights were flown to examine the atmosphere over the mixed wetland-woodland (taiga) terrain of northeastern Quebec (missions 11-20). Missions 1, 21, and 22 were transit flights over the northeastern United States. For a complete overview of ABLE 3B and a geographic map of the flight tracks, see *Harriss et al.* [this issue (a)].

1.1. *Atmospheric Nitric Acid*

Nitric acid is an important constituent in the photochemistry and acid-base chemistry of the troposphere. Almost all the NO produced during fossil fuel combustion is photochemically oxidized to NO_2 and then to HNO_3 [*Logan et al.*, 1983]. Nitric acid is very soluble in water and therefore is efficiently scavenged by wet deposition. In addition, HNO_3 is dry deposited in significant quantities to leaf surfaces [*Meyers et al.*, 1989]. It is still not known if HNO_3 is directly emitted from biomass-burning or exclusively produced from subsequent photochemical oxidation of NO_2. If HNO_3 is not directly emitted from a fire, significant amounts of HNO_3 must be rapidly produced given the enhanced mixing ratios of HNO_3 observed in fresh burning plumes [*LeBel et al.*, 1988; this study]. For a thorough discussion of the distribution and partitioning of HNO_3, peroxyacetyl nitrate (PAN), NO, NO_2, and other reactive odd nitrogen species measured over Canada during ABLE 3B, please refer to *Sandholm et al.* [this issue], *Singh et al.* [this issue], and *Talbot et al.* [this issue].

[1]Institute for the Study of Earth, Oceans, and Space, University of New Hampshire, Durham.
[2]School of Earth and Atmospheric Sciences, Georgia Institute of Technology, Atlanta.
[3]NASA Langley Research Center, Hampton.
[4]Department of Chemistry, University of California-Irvine, Irvine.
[5]Now at Fraunhofer-Institut für Atmosphärische Umweltforschung Garmisch-Partenkirchen, Germany.
[6]Now at Centralny Instytut Ochrony Pracy, Warsaw, Poland.

Paper number 93JD02091.
0148-0227/94/93-JD02091$05.00

1.2. *Atmospheric Formic and Acetic Acids*

Over the past 10 years it has been demonstrated that carboxylic acids are ubiquitous components of the global troposphere. *Keene et al.* [1983] found that HCOOH and CH_3COOH were the dominant acidity components of precipitation in remote regions, but these organic acids comprised only a minor portion of the free acidity in polluted regions. In general, gas phase carboxylic acids have a relatively short atmospheric lifetime, of the order of a few days due to removal by precipitation [*Keene and Galloway*, 1988] and dry deposition [*Talbot et al.*, 1988b]. Carboxylic acids have discernible seasonal and diurnal signals in the near-surface atmosphere, with the highest gas phase mixing ratios occurring during the summer and in the afternoon, respectively [*Talbot et al.*, 1988b].

Known sources of vapor phase carboxylic acids include direct emission from vegetation and soils, photochemical production from natural and anthropogenic hydrocarbons, biomass-burning, and vehicular emissions [*Arnts and Gay*, 1979; *Kawamura et al.*, 1986; *Keene and Galloway*, 1986; *Andreae et al.*, 1988b; *Jacob and Wofsy*, 1988; *Talbot et al.*, 1988b]. The seasonal and diurnal variations of carboxylic acid mixing ratios in the atmosphere indicate that natural sources, direct emissions and subsequent secondary production are important at midlatitudes [*Talbot et al.*, 1988b]. Biomass-burning may be a significant source of $HCOOH_{(g)}$ and $CH_3COOH_{(g)}$ to the atmosphere in some remote regions [*Talbot et al.*, 1988b; *Helas et al.*, 1992].

1.3. *Atmospheric Oxalate*

Oxalate $(COO^-)_2$ has been observed in cloud water, precipitation, and atmospheric aerosol particles in both polluted (White Face Mountain, New York) and remote regions of the Earth (Amazon basin, Brazil, and the North American Arctic) [*Norton et al.*, 1983; *Andreae et al.*, 1988a; *Talbot et al.*, 1988a; *Li and Winchester*, 1989; *Talbot et al.*, 1990c; *Cachier et al.*, 1991; *Lacaux et al.*; 1991; *Talbot et al.*, 1992]. *Andreae et al.* [1988a] found that biomass-burning plumes over the Amazon basin contained elevated levels of particulate phase $(COO^-)_{2\,(p)}$. In addition, $(COO^-)_{2\,(p)}$ measured by *Norton et al.* [1983] at a remote Colorado mountain site exhibited correlation with aerosol NO_3^- in polluted air masses.

While the work of *Andreae et al.* [1988a] indicated that atmospheric $(COO^-)_2$ may be naturally produced as a result of biomass-burning, it is still not certain if $(COO^-)_2$ is directly emitted from fires or is a secondary product. Anthropogenically derived $(COOH)_2$ may be a product of the gas or aqueous phase oxidation of glyoxal (CHOCHO) [*Norton et al.*, 1983], a compound that has been photochemically produced from aromatic hydrocarbons in smog chamber studies [*Nojima et al.*, 1974]. *Norton et al.* [1983] also suspected that their HNO_3 nylon filter gas-sampling system also collected small amounts of gaseous $(COOH)_2$ or gaseous oxalyl chloride ($(COCl)_2$), both of which become $(COO^-)_2$ in aqueous solution. Gaseous $(COCl)_2$ can be produced by oxidation of perchloroethylene (C_2Cl_4) by OH [*Howard*, 1976]. Thus far no one has been able to confirm the existence of gaseous $(COOH)_2$ in the atmosphere.

2. METHODS

2.1. *Gas Sampling*

Ambient air was brought inside the aircraft though a 4-cm ID ceramic-coated low-carbon (CCLC) steel inlet at a constant flow rate of 225 L/min. This inlet provided a constant flowing airstream from which the mist chamber, a water-soluble gas sampler, subsampled for acidic gases at a rate of 30-40 L/min. The CCLC inlet was mounted perpendicular to the aircraft, extending 30 cm out from the fuselage into the free airstream. The distance to the free airstream at this location on the aircraft is about 15 cm (NASA Global Troposphere Experiment (GTE) Project Office, NASA Langley Research Center, Hampton, Virginia, unpublished results, 1983). The CCLC steel inlet was tested in our lab and found to have 100% passing efficiency for HNO_3 and SO_2. We have not tested the passing efficiency of the inlet for carboxylic and oxalic acids. Given that experiments in our laboratory indicate that HNO_3 is more prone to inlet wall losses than carboxylic acids, it has been assumed that it has a passing efficiency of 100% for the CCLC inlet.

The CCLC steel inlet was not found to have any detectable "memory" effect (i.e., release of HNO_3 from the CCLC walls) while sampling "clean" air after 2-4 hours of exposure to 1-10 parts per billion by volume (ppbv) concentrations of HNO_3. Thus after flying through concentrated plumes and then back into "clean" air, we believe that acidic gases will not be released off the inlet walls influencing cleaner samples.

Water-soluble acidic gases were collected using the improved mist chamber technique [*Talbot et al.*, 1988b, 1990a, b]. The mist chamber, originally called a nebulization-reflux concentrator [*Cofer et al.*, 1985], uses a fine mist of water droplets to strip water-soluble atmospheric trace gases from a large volume of sampled air and concentrate them in a small aqueous volume (10 - 20 ml). Sampled air is pulled with a vacuum pump through a small diameter (1.5 mm) nebulizing nozzle which subsequently draws extracting solution (deionized water) through a second nozzle (1-2 mm) producing a fine mist within a glass chamber. The mist removes water-soluble gases from the airstream before the droplets are trapped by a hydrophobic membrane (Teflon filter) and drip back down into the reservoir of extracting solution. The large surface-area-to-volume ratio of the mist droplets results in efficient removal of soluble gases from the airstream into solution. The extracting solution can be analyzed by a variety of colorimetric or chromatographic techniques to quantify ions of interest in solution.

Ambient air samples were concentrated from 4 to 30 min at a flow rate of 30-40 slpm, as determined by an integrating linear mass flow meter (Teledyne Hastings-Raydist). Then, the integrated sample was withdrawn (~ 5 ml) from the mist chamber and placed in a 15-ml high density amber polyethylene bottle. An additional 5-ml rinse of deionized water was placed in the mist chamber and ambient air was sampled for 1 additional minute. The rinse water was removed from the mist chamber, added to the sample bottle, and the entire sample was immediately placed in an ice chest. As soon as possible, after each flight, the samples were preserved with $CHCl_3$ and analyzed for NO_3^-, $CHOO^-$, CH_3COO^-, and $((COO^-)_2)^{2-}$ within 24 hours of collection.

With one mist chamber we are able to measure the concentration of several different water-soluble gases at the same time. Most mist chamber samples were collected with a sampling resolution of 15 min (~0.5 m^3) depending on the flight profiles and inferred mixing ratios (high or low) based on real-time observations of CO, O_3, NO_x, and NO_y. The vast majority of the gas samples were obtained while flying at a constant altitude. Samples collected during vertical spirals had a resolution of 1000 - 2000 m. When operating the mist chamber on the Electra aircraft at altitudes above 4 km, where the ambient air temperature was below freezing, it was necessary to heat the glass exterior of the mist chamber 1°-2°C with resistance foil heaters to prevent ice from forming on the nozzles.

Sampling approximately every 15 min, we routinely measured nitric (HNO_3), formic (HCOOH), and acetic (CH_3COOH) acids. However, in certain air masses impacted by biomass-burning we also observed what appears to be gas phase oxalic ($(COOH)_2$) acid. The mist chamber collects HNO_3, HCOOH, and CH_3COOH with efficiencies of 100%, 98%, and 95%, respectively [*Talbot et al.*, 1988b; *Talbot et al.*, 1990a]. A collection efficiency for $(COOH)_2$ has not been determined, but given $(COOH)_2$ is very soluble in water, one could expect a fairly high collection efficiency for this acid [*Klemm and Talbot*, 1991].

Prior to each flight the mist chamber was cleaned by placing 10 ml of ultrapure deionized water in the mist chamber, pulling air though a carbonate/charcoal filter assembly to generate "clean" air, discarding the rinse water, and then repeating the process a number of times. The entire cleaning procedure took 2 hours and consisted of five short (3 min) rinses, followed by 10 long (10 min) rinses. The final two rinses were saved as blanks and treated in an identical manner to actual samples.

The carbonate/charcoal filter assembly consisted of two 47-mm carbonate-impregnated glass fiber filters and an activated charcoal filter cartridge followed by a Teflon filter. The carbonate filters remove all particles and acidic gases from the airstream, while the charcoal cartridge ensured that organic acids were completely removed from the cleaning airstream. The final Teflon filter collected any particles liberated from the charcoal cartridge. The carbonate-impregnating solution was 1.2 M Na_2CO_3 in a 5% glycerol/95% deionized water solution. Filters were impregnated just prior to the field mission. This process involved soaking the filters in the carbonate/glycerol solution and then drying them at 80°C for 100 min. They were taken to the field doubly sealed in polyethylene bags. Prior to each cleaning session, the carbonate/charcoal filter assembly was loaded with fresh carbonate filters. The charcoal cartridge lasted the whole field mission.

2.2. *Chemical Analysis*

Mist chamber samples were analyzed immediately after each aircraft mission in a field laboratory. Our field laboratory was set up in the student biochemistry labs at Canador College, North Bay, Ontario, and moved to the Aurora Hotel in Goose Bay, Newfoundland, when the Electra switched its base of operations.

Mist chamber samples were run on two independent Dionex ion chromatographic (IC) systems (inorganic anions and carboxylic acids) modified with manual Rheodyne 7010 injection valves. In addition, peristaltic pumps were used to transport the micromembrane suppressor chemical regenerant.

The anion IC was equipped with a Dionex Fast Anion column with 0.7 mM Na_2CO_3 /0.15 mM $NaHCO_3$ eluant and 25 mN H_2SO_4 as the suppressor regenerant. This anion system was used to quantify NO_3^- and $((COO^-)_2)^{-2}$. The carboxylic acids were quantified on a Dionex AS4 column using a 0.4 mM Na_2CO_3 eluant and 25 mN H_2SO_4 suppressor regenerant. Both systems have an analytical precision of 3-5 % for the species of interest here.

During ABLE 3B the mist chamber/ion chromatography (MC/IC) gas-sampling system had average detection limits of 60 parts per trillion volume (pptv) HCOOH, 90 pptv CH_3COOH, 10 pptv HNO_3, and 10 pptv $(COOH)_2$, assuming an average solution volume of 13.3 ml, an average sampled air volume of 0.5 m^3, and analytical detection limits (in μmol/L) of 0.1 ($HCOO^-$), 0.15 (CH_3COO^-), 0.02 (HNO_3), and 0.02 ($(COO^-)_2$). The mist chamber blanks never contained a significant level of any of the species of interest. The uncertainties assigned to the atmospheric mixing ratios reported for MC/IC samples were calculated using a propagation of errors that placed equal weighting on the following components: analytical uncertainty, air volume measurement uncertainty, collection efficiency, and inlet passing efficiency. The reported mixing ratios of HCOOH and CH_3COOH have an overall uncertainty of ±15% and ±20% for both HNO_3 and $(COOH)_2$.

2.3. *Ancillary Measurements*

The ancillary chemical and meteorological measurements utilized here were obtained and are available from the ABLE 3B data archive at the NASA Langley Research Center, Hampton, Virginia. The CO

measurements collected in ABLE 3B were made with the differential absorption CO measurement (DACOM) instrument [*Sachse et al.*, 1987]. The high precision (5-s averaged) DACOM data were averaged over the 15- to 20-min sampling times of the integrated mist chamber gas samples.

The Georgia Institute of Technology (GIT) NO, NO_2, and NO_y (total reactive odd nitrogen) measurements were made with a two-photon/laser-induced fluorescence (TP/LIF) instrument that detects NO [*Sandholm et al.*, this issue]. Navigational and meteorological data, including altitude, latitude, longitude, and static air temperature, were collected at a 1-Hz sampling rate using the NASA/GTE turbulent air motion measurement system (TAMMS). The GIT and TAMMS data sets were merged to the sampling times of the University of New Hampshire (UNH) mist chamber and aerosol samples by averaging all the data points that fell within the start and stop times of a given sample. The CO and odd nitrogen mixing ratios reported here are the "merged" or averaged values. The entire NASA/GTE ABLE 3B data archive is available from the NASA/GTE project office (NASA Langley Research Center, Hampton, Virginia).

The hydrocarbon sampling and analysis was performed by the University of California-Irvine [*Blake et al.*, 1992]. About 20 different hydrocarbons and halocarbons were determined by gas chromatography on the 60 samples routinely collected for each flight [*Blake et al.*, this issue]. The hydrocarbon values reported for a particular UNH sample are the average of hydrocarbon samples collected between the start and the stop of the UNH sample. Since the grab sample values cannot be integrated over our sampling times, hydrocarbon values reported here for a particular combustion plume represent samples collected coincident with the peak CO mixing ratio.

Five-day backward isentropic air mass trajectories were used to indicate potential air mass source regions and transport pathways [*Shipham et al.*, 1992, this issue].

2.4. *Enhancement Factors*

Historically, biomass-burning emission factors have been defined as the amount of species X that is emitted per unit of biomass combusted [*Crutzen et al.*, 1979; *Talbot et al.*, 1988b]. This definition has been loosely applied to measurements of species X in biomass-burning plumes [*Andreae et al.*, 1988a; *Helas et al.*, 1992]. However, there are numerous and significant differences between measurements made directly above a fire and samples collected in an aged plume. To clarify the terminology here, we use the term enhancement factor to refer to measurements of species X in combustion plumes far away from the source, while emission factors reflect measurements of species X in combustion emissions at or very near the source.

Carbon dioxide and CO have both been used as measures of biomass combustion since the release of these species has been related to the amount of C in the fuel materials. Since CO was measured from the ABLE 3B Electra aircraft and CO_2 was not, the enhancement ratios reported here were normalized relative to CO and calculated as the unitless ratio $\Delta X/\Delta CO$. The individual plume numbers correspond to the missions in which the impacted air mass was encountered. Although there were often more than one mist chamber sample with elevated mixing ratios collected near a particular plume, many of these 10-to-20-min integrated samples were partially diluted with background air. As a result, the mist chamber sample coincident with the peak CO mixing ratio was selected as the most representative of the "plume" composition and the most suitable for use in determining a $\Delta X/\Delta CO$ enhancement factor. Plume enhancement factors were determined two different ways: (1) as the enhancement of species X (ΔX) in units of its molar mixing ratio (pptv) divided by the enhancement of CO (ΔCO) in pptv (see Table 1) and (2) as the slope of the linear regression relating the mixing ratio of species X (ppbv) versus the average mixing ratio of CO (ppbv) (see Table 2).

The ΔCO used in the $\Delta X/\Delta CO$ enhancement factor calculations was determined by integrating the CO enhancement of the plume sample above the minimum CO mixing ratio of that flight. To facilitate the integration of the CO enhancement, gaps in CO data were spanned by linearly connecting the endpoints of the gap. Mist chamber samples missing CO data coverage over more than 50% of their sampling interval were excluded from consideration as a plume sample. To enable comparison to other studies, the $\Delta X/\Delta CO$ enhancement factors were converted to $\Delta X/\Delta CO_2$ enhancement factors (Table 1) using an average subarctic boreal forest fire $\Delta CO/\Delta CO_2$ emission factor of 0.069 [*Cofer et al.*, 1988].

The species X versus CO slope enhancement factors were determined using the CO mixing ratio averaged over the start and stop times of the mist chamber sample. The regression slope enhancement factors were derived using all the mist chamber samples collected for a particular mission. Only those CO relationships with an r^2 correlation coefficient greater than 0.75 are included in Table 2.

3. RESULTS

3.1. *Enhanced Plume Mixing Ratios*

Enhanced mixing ratios of gaseous $(COOH)_2$, HCOOH, CH_3COOH, and HNO_3 were observed in association with biomass-burning plumes over the Canadian study regions. Examples of this relationship are illustrated using vertical composites from missions 6, 9, and 11 (Figures 1a,b,c), which show the coincidence of the maxima in the mixing ratios of these four acidic gases with that of CO. The combustion plumes studied here were encountered on missions 4, 6, 8, 9, 10, 11, 13, 16, and 22. The C_2Cl_4 mixing ratios for plumes 10, 16, and 22 (18-82 pptv) were significantly enhanced over the 12-14 pptv of C_2Cl_4

TABLE 1. Summary of ΔX/ΔCO Enhancement Factors

	Mission							Biomass Burning Avg.	Biomass Burning s. d.	Mission		
	4	6	8	9a	9b	11	13			10	16	22
Avg. CO (bkg), ppbv	96	108	100	107	107	119	88			128	88	89
Avg. CO (plume), ppbv	149	210	160	137	225	297	133			431	237	209
Averaged ΔCO, ppbv	53	102	60	30	118	178	45			303	149	120
Integrated ΔCO, ppbv	49	94	61	27	118	169	47			175	149	120
Avg. HNO_3 (bkg), pptv	17	100	43	49	49	35	71			62	78	68
HNO_3 (plume), pptv	282	509	242	275	715	54	148			605	864	3797
$\Delta HNO_3/\Delta iCO$	5.4E-03	4.3E-03	3.3E-03	8.3E-03	5.6E-03	1.1E-04	1.6E-03	4.1E-03	2.7E-03	3.1E-03	5.3E-03	3.1E-02
$\Delta HNO_3/\Delta CO_2$*								2.8E-04	1.9E-04	2.1E-04	3.6E-04	2.1E-03
Avg. $(COOH)_2$ (bkg)†, pptv	< 8	< 11	< 12	< 10	< 10	< 10	< 6			< 15	< 6	< 7
$(COOH)_2$ (plume), pptv	< 46	80	17	22	28	126	25			61	82	67
$\Delta(COOH)_2/\Delta iCO$		7.4E-04	9.7E-05	4.6E-04	1.6E-04	6.9E-04	4.0E-04	4.2E-04	2.6E-04	2.7E-04	5.1E-04	5.0E-04
$\Delta(COOH)_2/\Delta CO_2$*								2.9E-05	1.8E-05	1.8E-05	3.5E-05	3.4E-05
Avg. HCOOH (bkg), pptv	193	649	420	857	857	164	365			553	288	354
HCOOH (plume), pptv	1437	3728	3073	2521	3781	1550	3310			4034	4728	1700
ΔHCOOH/ΔiCO	2.5E-02	3.3E-02	4.4E-02	6.1E-02	2.5E-02	8.2E-03	6.2E-02	3.7E-02	2.0E-02	2.0E-02	3.0E-02	1.1E-02
$\Delta HCOOH/\Delta CO_2$*								2.5E-03	1.4E-03	1.4E-03	2.1E-03	7.7E-04
Avg. CH_3COOH (bkg), pptv	297	775	567	1035	1035	405	662			909	533	441
CH_3COOH (plume), pptv	1995	2811	2212	1646	4526	3339	2147			4228	3614	2132
$\Delta CH_3COOH/\Delta iCO$	3 4E-02	2.2E-02	2.7E-02	2.3E-02	3.0E-02	1.7E-02	3.1E-02	2.6E-02	6.0E-03	1.9E-02	2.1E-02	1.4E-02
$\Delta CH_3COOH/\Delta CO_2$*								1.8E-03	4.2E-04	1.3E-03	1.4E-03	9.7E-04

Read 5.4E-03 as 5.4×10^{-3}; bkg, background.

*Converted using $\Delta CO/\Delta CO_2 = 0.069$ for subarctic forest fires [Cofer et al., 1988].

†Reported values are average $(COOH)_2$ detection limit for "background" samples.

TABLE 2. Summary of Regression Slope Enhancement Factors

	Mission					
	6	9	11	13	16	22
			HNO_3 Versus CO			
Regression slope	3.9E-03	5.9E-03	*	*	4.7E-03	2.9E-02
r^2	0.82	0.84	0.19	0.40	0.88	0.89
P value	<0.0001	<0.0001	0.2	0.02	<0.0001	<0.0001
n	12	16	10	14	14	13
			HCOOH Versus CO			
Regression slope	*	*	*	5.4E-02	3.1E-02	1.2E-02
r^2	0.47	0.57	0.63	0.91	0.94	0.96
P value	0.01	0.0008	0.003	<0.0001	<0.0001	<0.0001
n	12	16	11	14	14	13
			CH_3COOH Versus CO			
Regression slope	1.7E-02	3.0E-02	1.5E-02	2.8E-02	2.0E-02	1.5E-03
r^2	0.78	0.88	0.88	0.91	0.96	0.95
P value	<0.0001	<0.0001	<0.0001	<0.0001	<0.0001	<0.0001
n	12	16	11	14	14	13

Asterisks, only slopes with r^2 values greater than 0.75 are reported.

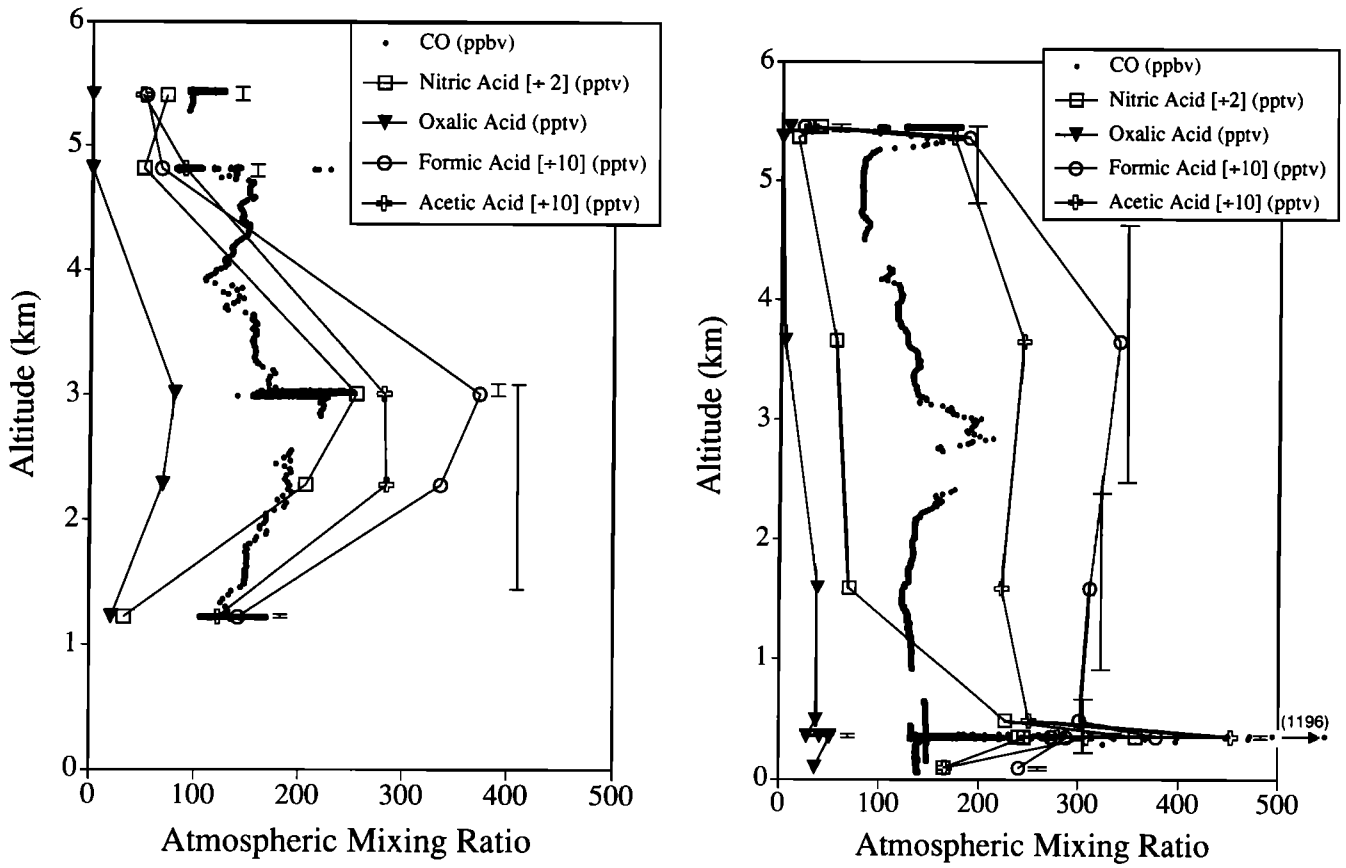

Fig. 1. Vertical composites from (a) mission 6 (1947-2130 UT), (b) mission 9 (2050-2233 UT), and (c) mission 11 (1448-1601 UT) showing elevated nitric and carboxylic acid mixing ratios in biomass- burning impacted air masses sampled at different altitudes. Bars represent altitudinal rage over which sample was collected.

measured for the other burning plumes (Table 3, Figure 2). Given that "background" air encountered in the Canadian subarctic during this mission contained 12-13 pptv of C_2Cl_4 [*Talbot et al.*, this issue], it is believed that only plumes 10, 16, and 22 were significantly impacted by anthropogenic activities. In addition, the 5-day backward isentropic air mass trajectories for plumes 10, 16, and 22 pass over highly industrialized regions of Canada and the United States, further suggesting potential anthropogenic influence on these air masses [*Shipham et al.*, this issue].

In the summertime, central and eastern Canada commonly receives air masses influenced by the urban, industrial, and agricultural centers to the west and southwest [*Harriss et al.*, this issue (b)]. However, with the exception of the pollution episodes encountered during missions 10 and 16, C_2Cl_4 and F 12 mixing ratios (Figure 2) suggest that very few, if any, of the other air masses encountered in Canada contained considerable amounts of urban or industrial pollution. Although, it is certainly likely that these regions experience episodic low-level inputs of anthropogenic pollution during the summer months.

As a group, the plume samples had an average composition statistically different from the average composition of the air in which the plumes occurred (Figure 3). The average "plume" mixing ratios of the acidic gases studied here were at least twice their average "background" values. In most cases they were 4 times greater. Note that gaseous $(COOH)_2$ was below detection in "background" air, therefore the "plume background" $(COOH)_2$ mixing ratio reported in Figure 3 is the average $(COOH)_2$ detection limit for the "background" samples.

The principal source of atmospheric CO enhancements over the Canadian study regions was from combustion processes [*Harriss et al.*, this issue (a, b)]. Correlation coefficients were calculated for the relationship between various species and the average CO mixing ratio for a given gas-sampling interval (Table 2). Of the four gases discussed here, CH_3COOH was the one most highly correlated with CO (i.e., $r^2 > 0.75$, $P < 0.0001$) over the most missions (e.g., missions 6, 9, 11, 13, and 16) (see Table 2). Individual CO correlations for HNO_3, HCOOH, and CH_3COOH from various missions are displayed as examples in Figure 4. A combined CO to $(COOH)_2$ correlation for missions 11, 16, and 22 is included in Figure 4. It was not possible to calculate a $(COOH)_2$ correlation for individual missions due to the small number of samples for which $(COOH)_2$ was detectable.

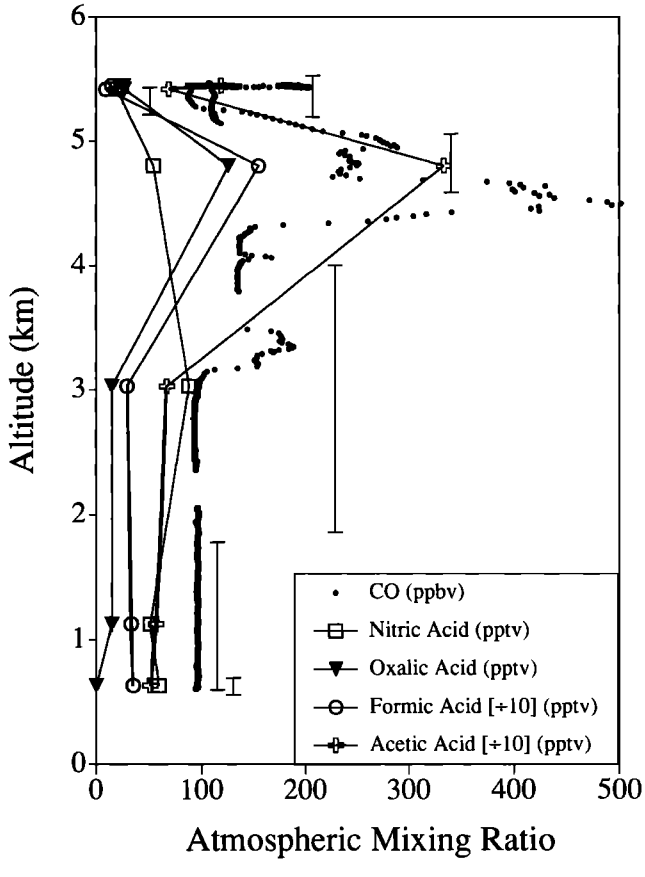

Fig. 1. (continued)

3.2. *Enhancement Factors*

The $\Delta X/\Delta CO$ enhancement factors of $(COOH)_2$ were 3 orders of magnitude less than $\Delta X/\Delta CO$ enhancement factors for HCOOH and CH_3COOH (Figure 5). While $\Delta HCOOH/\Delta CO$ enhancement factor values appear to be twice those of CH_3COOH in plumes 9a and 13, these two carboxylic acids were enhanced in nearly equal amounts in plumes encountered on missions 6, 9b, 10, and 22.

The average of the $\Delta X/\Delta CO$ enhancement factors for the biomass-burning plumes were (average ±s.d.): HNO_3 ($4x10^{-3}$ $\pm 3x10^{-3}$); $(COOH)_2$ ($4x10^{-4}$ $\pm 3x10^{-4}$); HCOOH ($4x10^{-2} \pm 2x10^{-2}$); and CH_3COOH ($3x10^{-2} \pm 6x10^{-3}$). The less than twofold variation associated with these average $\Delta X/\Delta CO$ enhancement factors are quite comparable to other $\Delta X/\Delta CO$ values for these species reported in the literature [e.g., *Andreae et al.*, 1988a; *Talbot et al.*, 1988b] and indicate that there was relatively little difference in enhancement factor values for the suite of biomass-burning impacted air masses sampled over Canada. Some of the lowest $\Delta(COOH)_2/\Delta CO$ ratios were measured on missions 8, 9b, and 10.

The $\Delta X/\Delta CO$ and the regression slope methods of determining plume enhancement factors compared very well, yielding a correlation coefficient of 0.99 ($P < 0.0001$) (Figure 6). Although on average the regression slope technique yielded slightly larger enhancement factor values, this minor difference is well within the uncertainty of the $\Delta X/\Delta CO$ calculations and is strongly influenced by one value (Figure 6). Given the similarity of two techniques and the fact that it was possible to calculate enhancement factors for more of the plumes with the $\Delta X/\Delta CO$ technique, most further analysis and discussion in this paper utilizes $\Delta X/\Delta CO$ values.

TABLE 3. Summary of Plume Characteristics (Average Mixing Ratios Over UNH Sampling Times)

Plume	Avg. Sample Altitude, km	Average CO, ppbv	Average NO_x, pptv	Average NO_y, pptv	F12, pptv	C_2Cl_4, pptv	Potential Source Regions*	Potential Air Mass Modifications*
4	1.6	149	127	1440	497	13	Canada	local biomass burning, western Ontario
6	3.0	201	38	1906	506	14	Alaska	remote biomass burning
8	1.2	160	60	587	500	12	central Canada	local biomass burning
9a	1.1	134	81	582	----	----	central Canada	local biomass burning pollution
9b	0.4	225	1197	2570	489	12	central Canada	local biomass burning
10	2.8	431	2737	5480	490	20	central United States	pollution, rain local biomass burning
11	4.8	297	47	5350	497	12	North Pacific Canada	local and remotebiomass burning rain
13	2.0	135	30	341	489	13	North Atlantic	remote biomass burning pollution, rain
16	0.3	237	135	684	495	18	maritime provinces	remote biomass burning pollution, rain
22	0.2	209	429	3980	547	82	central-southern United States	pollution

UNH, University of New Hampshire.
*From ***Shipham et al.*** [this issue].

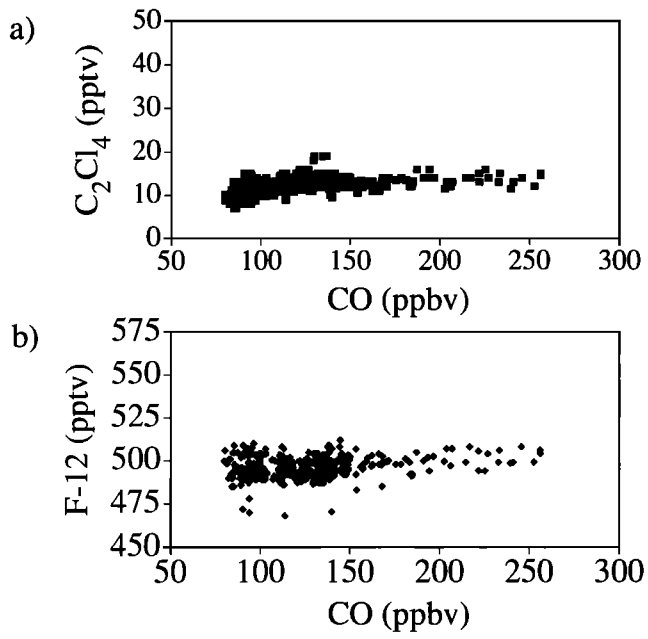

Fig. 2. Comparison of C_2Cl_4 and F 12 mixing ratios to CO in biomass burning impacted air masses (i.e., all samples from plume missions, except missions 10, 16, and 22, which showed obvious anthropogenic influences).

3.3. *Plume Characteristics*

A summary of the ancillary chemical and meteorological parameters of each of the plumes discussed in this study can be found in Table 3. Parts of this table are based on a study by *Shipham et al.* [this issue] who identified potential source regions of the biomass-burning plumes using 5-day backward isentropic air mass trajectories. Likely modifications to the sampled air masses during atmospheric transport are also listed in Table 3. To better understand the nature of the plumes sampled in this experiment and to interpret the calculated enhancement factors, a brief description of each plume follows:

Plume 4. A relatively fresh biomass-burning plume probably originated from western Ontario. For several days prior to the mission, the northern Ontario region was probably influenced by anthropogenic air, as indicated by enhanced $SO_4^{2-}{}_{(aero)}$ levels in the Kinosheo Lake region [*Harriss et al.*, this issue (b)]. While most of the upper level trajectories indicated a Canadian source region, the low-level trajectories originated in the United States, supporting a possible anthropogenic influence. The modest CH_4 increase in this plume suggests efficient combustion [*Harriss et al.*, this issue (b)]. This plume appears to be one of the freshest ones sampled, as indicated by the presence of the short-lived 1,3-butadiene, not found in most other plumes [*Blake et al.*, this issue].

Plume 6. A high-altitude plume was encountered over western Manitoba/eastern Saskatchewan that was traced back to a region of Alaska [*Shipham et al.*, this issue] where extensive forest fires were occurring [*Shipham et al.*, this issue]. This plume appears to be a good example of rapid long-range transport (4-5 days) with little air mass modification along the way (see also Figure 1a).

Plume 8. A fresh tundra fire plume was sampled at 1 km altitude. Tower-based aerosol data from Fraserdale suggest that missions 8 and 9 occurred on the second or third day of a 6-day anthropogenic pollution event [*Harriss et al.*, this issue (b)]. In addition, *Harriss et al.* [this issue

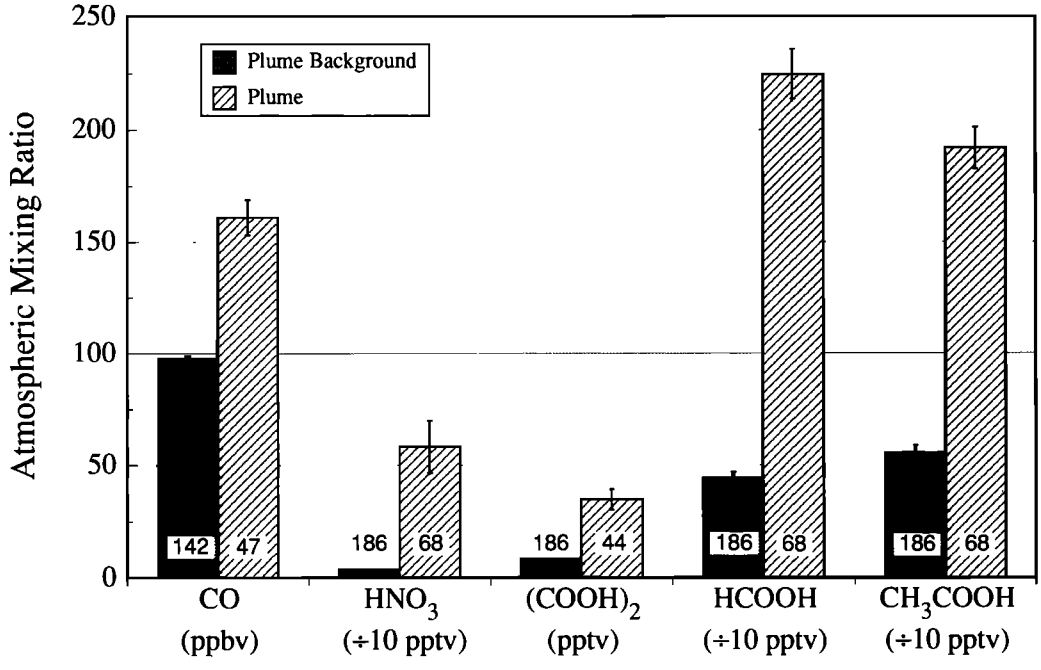

Fig. 3. Comparison of the average "plume" mixing ratios with average "plume background" mixing ratios. Number near base of bar indicates number of samples averaged. $P < 0.0001$ for all species.

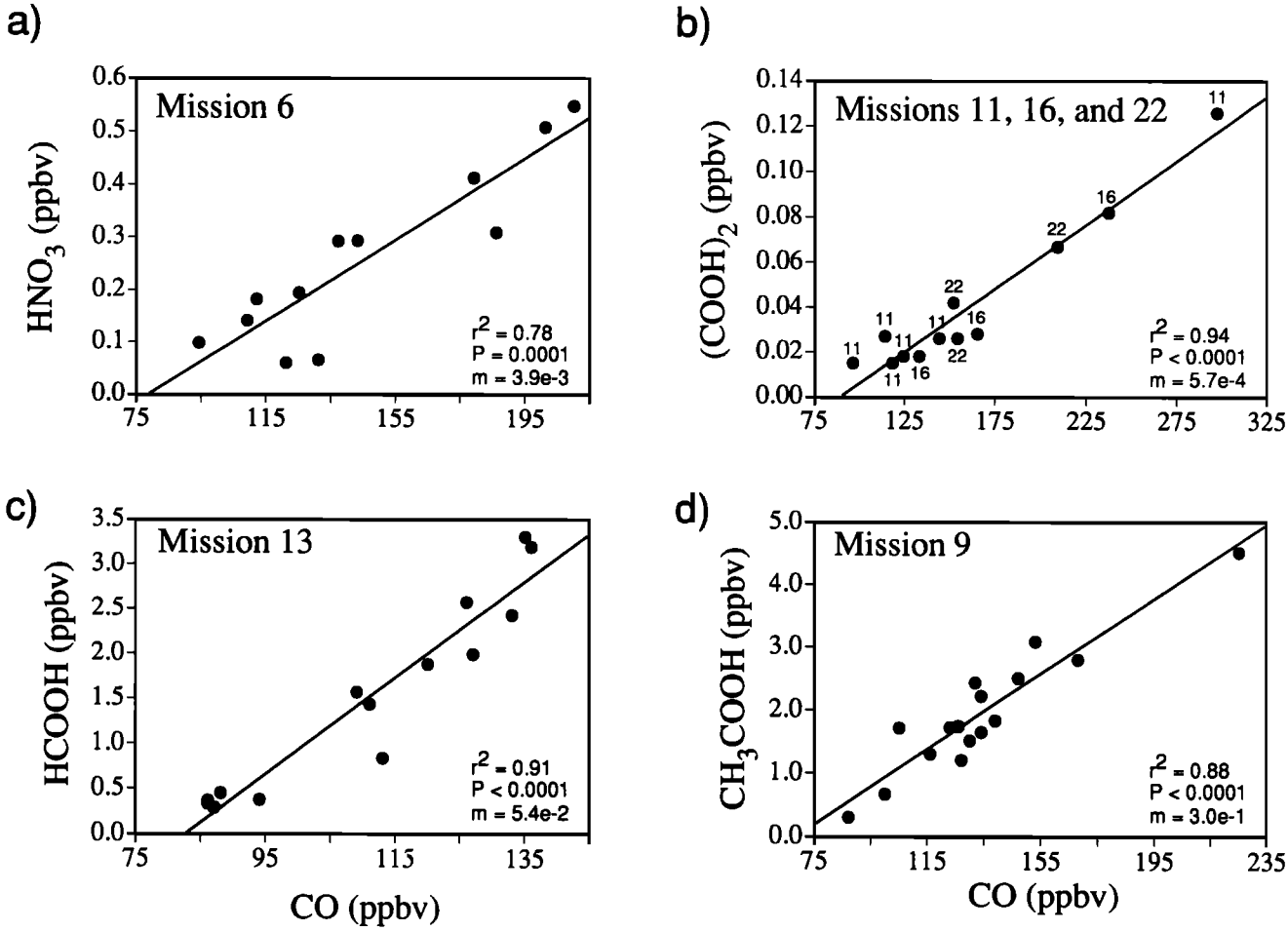

Fig. 4. Relationship among (a) HNO_3, (b) $(COOH)_2$, (c) HCOOH, and (d) CH_3COOH and CO for selected missions.

(b)] reported discrete "layers" with a wide range of $\Delta CH_4/\Delta CO$ ratios, suggesting air masses from different sources. The ultraviolet differential absorption lidar (UV DIAL) data of *Browell et al.* [this issue] showed enhanced O_3 mixing ratios in these "layers," without elevated aerosol concentrations, indicating some air mass modification during transport (e.g., precipitation scavenging of aerosols).

Plume 9a. Just outside of North Bay, while in transit to Kinosheo Lake, this plume was encountered at an altitude of 1 km. Mission 9 occurred on the same day as mission 8, so the mixed source regions discussed above for plume 8 also apply here. Visible satellite imagery showed widespread smoke/haze over northern and western Ontario, while the Moosonee ground site reported elevated smoke layers. The air mass trajectories for this plume traveled near the Sudbury smelter. The aerosol sample from this plume had one of the highest SO_4^{2-} mixing ratios of this field campaign [*Gorzelska et al.*, this issue].

Plume 9b. This was probably the freshest biomass-burning plume sampled during ABLE 3B, although there are no hydrocarbon samples in the plume to confirm this. The aircraft sampled a small (~10 ha) flaming tundra fire at 350 m altitude. Behind a flaming front the already burned, smoldering areas provided secondary inputs of CO-enriched air. The plume was trapped at the top of the mixed layer (1 km). This was the same biomass-burning source sampled 7 hours earlier on mission 8, but this time much closer to the source (see also Figure 1*b*).

Plume 10: Midaltitude plume, which had been convectively pumped to the aircraft's 2.7 km altitude, was sampled near Schefferville. Lower-level air mass trajectories indicated the possible influx of emissions from a regional tundra fire with probable modification of the sampled air mass due to precipitation. However, elevated C_2Cl_4 mixing ratios and middle and upper air mass trajectories indicate the advection of fresh pollution from the Great Lakes region of the United States [*Shipham et al.*, this issue] associated with a cold front to the west of Schefferville [*Bakwin et al.*, this issue]. In addition, some of the highest aerosol SO_4^{2-} mixing ratios of ABLE 3B were observed in this plume.

Plume 11. Sampling was conducted in a high-altitude (5 km) haze layer over the Schefferville area. Regional rawinsonde reports revealed inversions which could have trapped aged smoke from fires in western and central Canada. Upper level trajectories showed flows coming

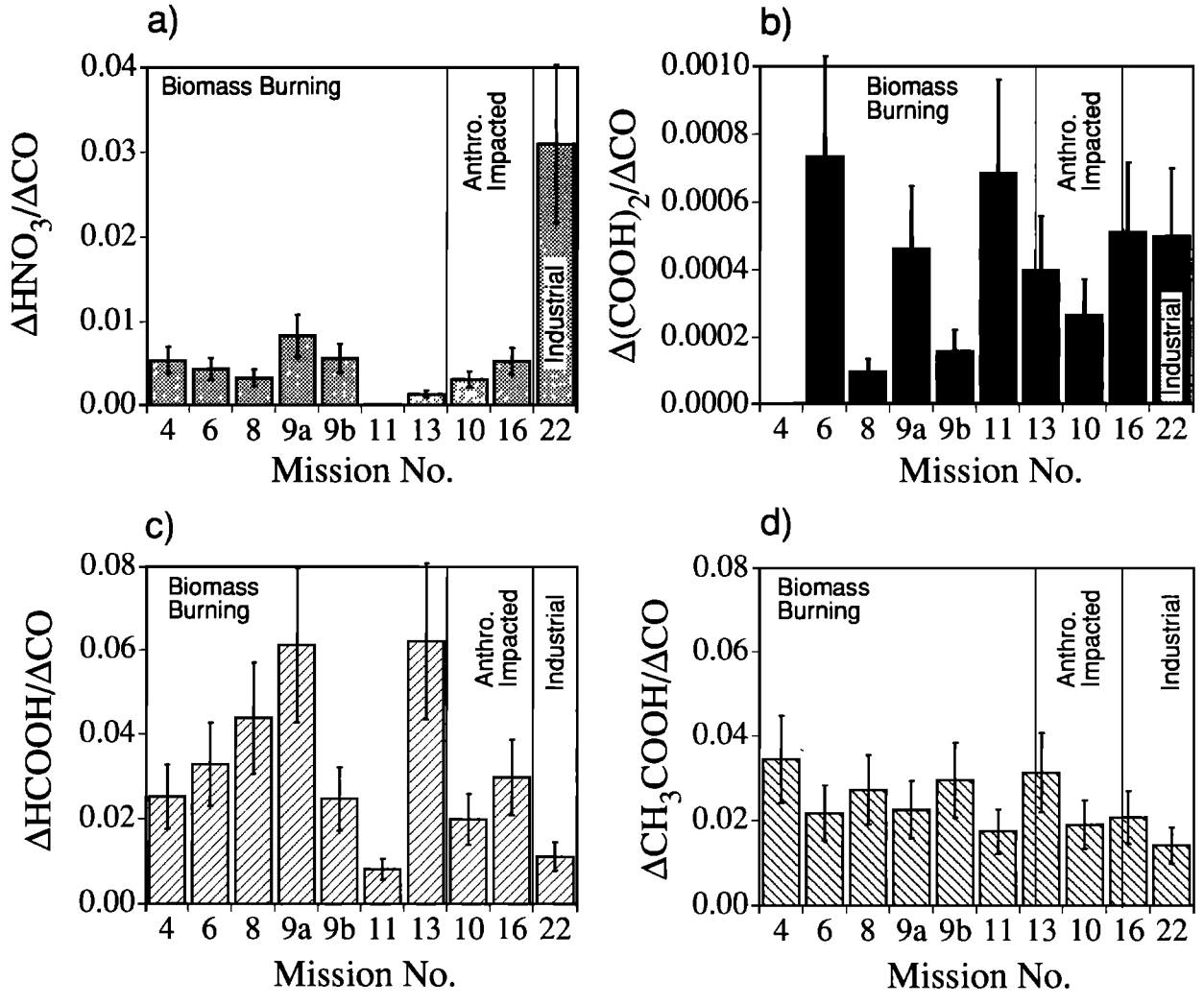

Fig. 5. $\Delta X/\Delta CO$ enhancement factors for each combustion- impacted air mass (a) HNO_3, (b) $(COOH)_2$, (c) HCOOH, and (d) CH_3COOH.

into the region from over both the Gulf of Alaska and the Arctic Ocean. Low-level winds were dominated by Hurricane Bertha off the New England coast (see also Figure 1*c*).

Plume 13. Pronounced haze layer at 2 km altitude that visible satellite imagery indicated was covering the entire region. Most of the trajectories originated in western Canada, although a couple point to the north central United States, suggesting a possible pollution influence on aged biomass-burning haze.

Plume 16. In this case a low-altitude plume was sampled over the Atlantic Ocean. This plume appears of have been sealed off from the free troposphere by a strong inversion that capped the top of the boundary layer at 3 km. Elevated $C_2Cl_{4\,(g)}$ and aerosol SO_4^{2-} mixing ratios corroborate with the trajectories implying a pollution source from the Canadian maritime provinces (e.g., Halifax, Newfoundland).

Plume 22. An aged anthropogenic pollution plume that had experienced little or no rainout was sampled at 250 m altitude over the ocean along the eastern coastline of Virginia. Mixing ratios of F 12, C_2Cl_4, and aerosol SO_4^{2-} were very high, the highest SO_4^{2-} of ABLE 3B. This plume did not impact Canadian air masses and had an origin in the middle and south central United States, as indicated by air mass trajectories.

Plume groupings. Plumes 4, 8, and 9b represented fresh biomass-burning plumes, while plumes 6 and 11 were probably aged plumes. The only indication of significant anthropogenic influence were the elevated C_2Cl_4, F 11, F 12, F 113, and SO_4^{2-} mixing ratios detected during the last half of mission 22 and portions of missions 10 and 16. The plume encountered in the beginning of mission 9 (plume 9a) is also suspected to have an urban/industrial influence since it also had elevated SO_4^{2-} mixing ratios; unfortunately, hydrocarbon samples were not collected in this plume.

Plumes were also observed on other missions, particularly missions 7, 12, 17, 20, and 21. These missions were not included in this analysis for a variety of reasons,

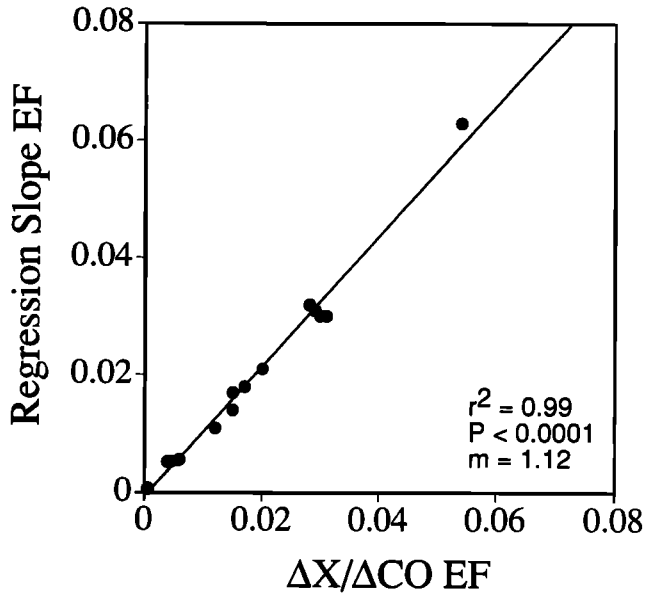

Fig. 6. Regression slope enhancement factors (EF) compared to ΔX/ΔCO enhancement factors.

the foremost being insufficient data coverage. In addition, many of the plumes that are not included in this analysis were not discretely captured with our 15-min sampling resolution and as a result diluted with background air to such a degree that a meaningful enhancement factor could not be calculated.

4. Discussion

4.1. *Enhancement Factors*

Since CO is produced from incomplete combustion, the amount of CO emitted during biomass-burning is a function of the fire conditions. Almost all of the CO is emitted during the smoldering stage of a fire, where as much as 20% of the combusted C is emitted as CO [*Crutzen et al.*, 1985]. Hot flaming fires, on the other hand, are not O_2 starved and produce much less CO. Since CO has a relatively small mixing ratio in the remote atmosphere (i.e., ≤ 100 ppbv), a chemical lifetime of several months, is generally passive to removal by depositional processes, and is not involved in biological respiration, CO is generally thought to be one of the more appropriate species to which biomass-burning plume enhancements are ratioed [*Andreae et al.*, 1988]. However, CO can be produced via the incomplete oxidation of hydrocarbons in biomass-burning [*Wofsy et al.*, this issue], so ΔX/ΔCO enhancement factors may be a slight under estimate of the amount of species X produced per unit of carbon in the original fuel. In any case, ΔX/ΔCO ratios are more suitable than $\Delta X/\Delta CO_2$ as emission factors for the smoldering stages of a fire [*Wofsy et al.*, 1992; *Crutzen and Andreae*, 1990].

Emissions from hotter, flaming fires are more likely to be transmitted to higher altitudes initially and are therefore more likely to be transported long distances. After the primary fire, emissions from smoldering fires could also be lifted to higher altitudes by vertical convective processes. Days later, after mixing in transport, it may be difficult to distinguish if an air mass is a product of a flaming or smoldering fire. In either case, these air masses should probably be classified as biomass-burning impacted rather than biomass-burning plumes.

It is important to consider that even for the fresh plumes, a 10-min sampling resolution will not provide peak emission ratios, since the aircraft was not necessarily in the fresh plume the entire time. Dilution with background air does occur during the collection of plume samples at these temporal resolutions. In this respect, the regression slope technique of calculating enhancement factors may be a more appropriate method, assuming one still obtains a sufficient number of measurements to get a meaningful regression. In either case, for those species that are directly emitted during combustion, an enhancement factor can be viewed as a lower limit of the actual emission factor, considering the many removal mechanisms or reactions which may influence a particular species over time. It is more ambiguous as what an enhancement factor actually represents for the species that are produced in the plumes during transport, as is believed to occur in the case of HCOOH [*Helas et al.*, 1992].

4.2. *Enhancement Factors As a Function of Plume Characteristics*

Despite having varying ages and sources, there is relatively little variability in the biomass-burning enhancement factor values for the different plumes (Figure 5, Table 1). The relatively small difference between the enhancement factors for the biomass-burning plumes and the anthropogenically impacted plumes (missions 10 and 16) could lead one to conclude that during transit across the North American continent to Canada, both anthropogenic and natural processes are injecting combustion products into these air masses. Subsequently, the combustion products sampled in these plumes cannot be easily attributed to one source.

The comparison of emission characteristics related to biomass-burning versus anthropogenic/urban sources is best illustrated by these two extremes: a fresh bog fire (plume 9b) and an aged plume of industrial pollution off the eastern coast of the United States (plume 22). It is important to note that plume 22 did not impact Canadian air masses. The anthropogenic $\Delta HNO_3/\Delta CO$ enhancement factor (plume 22) is approximately 6 times higher than any other HNO_3 enhancement factor (Figure 5), indicating that HNO_3 may be much more efficiently produced in urban combustion plumes. Nevertheless, biomass-burning is still a primary source of HNO_3 to the

subarctic Canadian troposphere in the summertime [*Talbot et al.*, this issue].

A similar comparison of $(COOH)_2$ enhancement factors for plume 22 suggests that urban/industrial combustion may also be an important source of gaseous $(COOH)_2$. In contrast, HCOOH appears to have higher enhancement factors in the biomass-burning plumes than in the industrial plume. This rough comparison of natural and anthropogenic sources does not show a clear trend for CH_3COOH.

4.3. *Comparison of Fresh and Aged ABLE 3B Plumes*

Another potentially useful comparison is to see how the chemical composition of fresh differ from more aged biomass-burning emissions. A higher enhancement factor in an aged plume would indicate that a species may be produced by secondary chemical reactions during transport. A lower enhancement factor value in aged plumes suggests an influence from removal mechanisms, such as washout of soluble species or chemical decomposition. Certainly many homogeneous and heterogeneous chemical reactions (e.g., acid/base, photochemical, gas-to-particle conversion) are occurring during transport.

Unfortunately, there is not an established reliable method of determining the relative age of a biomass-burning plume. However, it is possible to crudely discriminate the relative age of a few plumes using plume 9b as a fresh plume and plumes 6 and 11 (plumes encountered at higher altitudes (>3 km)) as more aged examples. Using this first-order age classification, there is no significant difference among the HNO_3, HCOOH, and CH_3COOH $\Delta X/\Delta CO$ enhancement factors from plume 9b (fresh) and plumes 6 and 11 (more aged). An exception to this rule is plume 11, which had a much lower $\Delta HNO_3/\Delta CO$ and $\Delta HCOOH/\Delta CO$ enhancement factor values (Figure 5), however it is unclear what process would remove HNO_3 and HCOOH, while not depleting CH_3COOH and $(COOH)_2$. On the other hand, the $\Delta(COOH)_2/\Delta CO$ enhancement factors for missions 6 and 11 are much larger than the $(COOH)_2$ enhancement factor from plume 9b (Figure 4), suggesting that $(COOH)_2$ may be produced in biomass-burning plumes by secondary chemical reactions.

Andreae et al. [1988a] used the NO/CO ratio as a measure of plume age, assuming that the NO would be converted to HNO_3 as the plume aged. In general, a higher ratio value of NO/CO indicates younger plumes, although the temperature of the combustion process is also a factor (i.e., flaming fires have relatively more NO and less CO, whereas smoldering fires produce relatively less NO and more CO). NO_x was used relative to CO here instead of NO, to remove the uncertainties due to rapid photochemical cycling between NO and NO_2 reservoirs. In this study, plumes 9b, 10, and 22 had elevated NO_x/CO ratios (Figure 7). It is not surprising

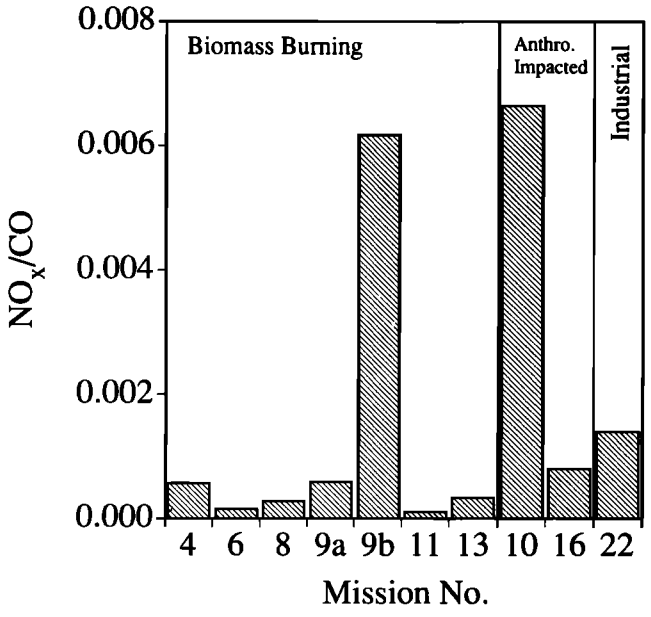

Fig. 7. NO_x/CO ratio for various combustion plumes.

that plume 9b had a high NO_x/CO ratio value since these data were collected close to a tundra fire. The fairly low NO_x/CO ratio for plume 22, an obvious urban/industrial plume, suggests that the anthropogenic emissions sampled on this mission could have been aged a few days. Plume 10, with its very large NO_x/CO ratio, was probably a mixture of fresh biomass-burning and anthropogenic emissions. Trajectories for plume 10 revealed that the air masses had recently passed over large midwestern urban areas of the United States [*Shipham et al.*, this issue].

Although the NO_x/CO ratio readily indicates the presence of fresh combustion emissions, it does not appear to be useful for finer plume age discrimination. Once the plumes age 2-3 days, the NO_x mixing ratios are indistinguishable from "background" air values [*Talbot et al.*, this issue].

Even ratios among various hydrocarbons appear to yield ambiguous information about the age of various biomass-burning plumes [*Sandholm et al.*, this issue]. However, *Blake et al.* [this issue] point out that 1,3-butadiene, primarily detected in plumes 4 and 9b, appears to be a good indicator of fresh biomass-burning emissions. This short-lived alkene should prove to be useful; unfortunately, there is still no good method of determining the age of a plume that is older than a few hours, making it difficult to unravel the chemical transformations occurring as the plume ages (see section 4.6).

4.4. *Enhancement Factors Compared to Previous Work*

LeBel et al. [1988] report an average $\Delta HNO_3/\Delta CO_2$ enhancement factor of 1.2×10^{-4} from fresh wetland smoke plumes in southern Florida, which compares well with the work of *Andreae et al.* [1988a]. In fresh and aged

haze layers over Amazonia during ABLE 2A, $\Delta HNO_3/\Delta CO_2$ ratios were 1 x 10^{-4} to 5 x 10^{-4}. In this study, the fresh and aged enhancement factors were also similar. The average ABLE 3B biomass-burning $\Delta HNO_3/\Delta CO$ enhancement factor converts to an approximate $\Delta HNO_3/\Delta CO_2$ ratio of 3 x 10^{-4} ±2 x 10^{-4} (assuming an average and constant subarctic boreal forest and tundra $\Delta CO/\Delta CO_2$ emission ratio of 0.069 [*Cofer et al.*, 1988]).

The fact that both fresh and aged biomass-burning plumes had similar HNO_3 enhancement factors could suggest that HNO_3 is efficiently produced in biomass-burning plumes. Alternatively, the similarity of these enhancement factors could indicate the direct emission of significant HNO_3 from biomass combustion. However, combustion plumes appear to provide an efficient chemical environment for conversion of NO_x to other NO_y species [*Jacob et al.*, 1992]. The only HNO_3 enhancement factor significantly different, an order of magnitude larger in value than those previously measured, was observed over the industrial eastern United States (mission 22). Again we emphasize the fact that this plume did not impact the subarctic regions of Canada.

The only published biomass-burning emission factors for HCOOH and CH_3COOH are for laboratory fires determined by *Talbot et al.* [1988b] and *Hartmann* [1990]. Both groups measured the carboxylic acid, CO, and CO_2 mixing ratios from 0.5 m [*Talbot*] and 2 m [*Hartmann*] above the fire. *Talbot et al.* [1988b] burned various types of biomass (hardwood, dried brush, leaves, and green brush), while *Hartmann* [1990] combusted hay and documented the trace gases emitted during the different phases of a fire. These two carboxylic acids were also measured in biomass-burning plumes over the northern Congo rain forest during the Dynamique et Chimie de l'Atmosphère en Forêt Equatoriale (DECAFE) [*Helas et al.*, 1992] and over the Venezuelan savanna [*Hartmann*, 1990]. Although *Helas et al.* [1992] did not report enhancement factors, we calculated approximate $\Delta HCOOH/\Delta CO$ enhancement ratios from the data provided in their paper.

The "laboratory" emission factors of 1.7 x 10^{-4} ±2.7 x 10^{-4} [*Talbot et al.*, 1988b] and 2.6 x 10^{-3} ±2 x 10^{-3} [*Hartmann*, 1990] are 1 to 2 orders of magnitude smaller than the $\Delta HCOOH/\Delta CO$ biomass-burning enhancement factors observed in ABLE 3B (3.5 x 10^{-2} ±2.2 x 10^{-2}) and DECAFE (~ 2 x 10^{-2}). The average $\Delta CH_3COOH/\Delta CO$ enhancement ratios for the ABLE 3B (2.6 x 10^{-2} ±6.8 x 10^{-3}) and DECAFE (8 x 10^{-3} ±4 x 10^{-3} (Congo)), and Venezuelan (3.2 x 10^{-3}±4 x 10^{-4}) expeditions were somewhat larger (1-10 times) than the "laboratory" $\Delta CH_3COOH/\Delta CO$ emission factors of 1.6 x 10^{-3}±2.4 x 10^{-3} [*Talbot et al.*, 1988b] and 8.7 x 10^{-3} ±6.1 x 10^{-3} [*Hartmann*, 1990] (see Figure 8). The difference between carboxylic acid emission factors determined in burning experiments and enhancement factors measured in actual biomass-burning plumes may be a function of different fuels or fire conditions (i.e., smoldering versus flaming).

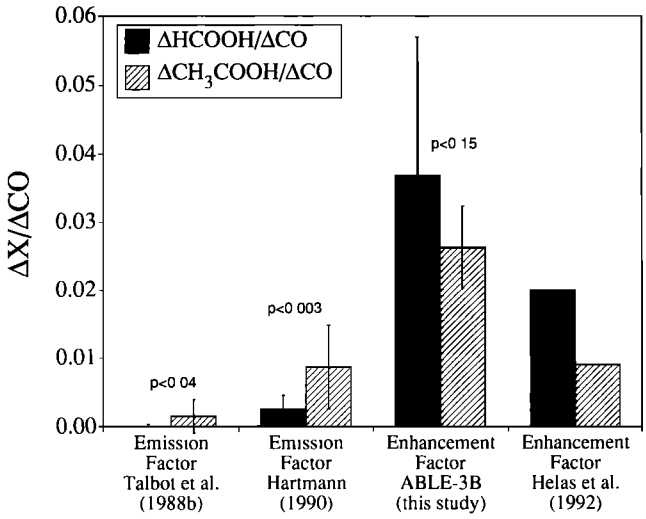

Fig. 8. Relationship between HCOOH and CH_3COOH in laboratory-determined emission factors and actual plume enhancement factors.

Certainly, over Canada, many plumes were the result of smoldering fire emissions. The observed enhancement factors in these plumes are supported by the faster release rates of carboxylic acids during smoldering stages of fires [*Hartmann*, 1990]. In addition, larger plume enhancement factors may actually indicate that HCOOH and, to a lesser degree, CH_3COOH are being produced secondarily in the plume (see section 4.5).

Considering the different fuels burned (tundra/boreal forest versus tropical rain forest), the close agreement between our enhancement factors and the approximate values from the DECAFE data is interesting. In addition, the average plume HCOOH and CH_3COOH mixing ratios (3.7 ±1.0 and 2.7 ±0.9 ppbv, respectively) reported by *Helas et al.* [1992] for DECAFE are similar to the plume mixing ratios observed during ABLE 3B (2.8 ±1.1 and 2.8 ±1.0 ppbv, respectively).

4.5. *Secondary Carboxylic Acid Production*

Talbot et al. [1988b] documented that different natural and anthropogenic carboxylic acid sources had different $HCOOH/CH_3COOH$ ratios. In burning experiments, *Hartmann* [1990] and *Talbot et al.* [1988b] reported $HCOOH/CH_3COOH$ ratios of 0.3 and 0.1, respectively. However, the average ratio of the plume mixing ratios of these two acids were 1.0 during ABLE 3B and 1.4 for DECAFE [*Helas et al.*, 1992]. *Helas et al.* [1992] point out that ratio of the enhancement factors, i.e., $\Delta HCOOH/\Delta CO$ to $\Delta CH_3COOH/\Delta CO$ (1.3 and 1.8 for ABLE 3B and DECAFE, respectively), may be more appropriate than comparing ratios of mixing ratios, (i.e., $HCOOH/CH_3COOH$). Indeed, enhancement factors represent the amount of enhancement in the plume over "background" air values. Both types of $HCOOH/CH_3COOH$ ratios highlight the difference

between fresh and aged biomass-burning emissions. The results of the fresh burning experiments in the laboratory portray CH_3COOH as the primary carboxylic acid emitted from biomass-burning, while combustion plumes encountered over North America, South America, and Africa contain HCOOH at mixing ratios equal to or greater than those of CH_3COOH. The fact that enhancement factors from fresh biomass-burning plumes (missions 4 and 6) also exhibited this enhancement of HCOOH over CH_3COOH (Figure 9), implies that if HCOOH is produced via secondary chemical reactions in the plume, it occurs fairly soon after emission.

Sanhueza et al. [1989] noticed that precipitation collected during periods of savanna burning in Venezuela had higher concentrations of HCOOH and CH_3COOH than precipitation collected during nonburning periods. Similarly, *Sanhueza* [1991] noted that the biomass-burning impacted precipitation had concentrations of HCOOH about 1.5 times higher than CH_3COOH. They concluded that the difference between the $HCOOH/CH_3COOH$ ratios of biomass-burning impacted precipitation and the laboratory-burning ratios of *Talbot et al.* [1988b] could be attributed to "atmospheric processes" rather than direct emission. *Helas et al.* [1992] also recognized this disparity and proposed that carboxylic acids (predominately HCOOH) are being produced in the biomass-burning plumes via the oxidation of olefins by O_3.

5. CONCLUSION

Carboxylic acid (HCOOH and CH_3COOH) enhancement factors and plume mixing ratios compared well to those observed in biomass-burning plumes over equatorial Africa (DECAFE experiment). Similarly, the calculated biomass-burning $\Delta HNO_3/\Delta CO_2$ ratios appear to agree with enhancement ratios measured previously. The $HCOOH/CH_3COOH$ ratios observed during ABLE 3B and DECAFE attest to secondary production of HCOOH in fire plumes when compared to ratios in "fresh" biomass-burning emissions determined from laboratory experiments. However, the similarities between the enhancement factors of the "fresh" (e.g., plume 9b) and the "aged" (e.g., plume 6) plumes encountered on ABLE 3B suggest that the HCOOH production in the plumes occurs in the first couple hours after emission.

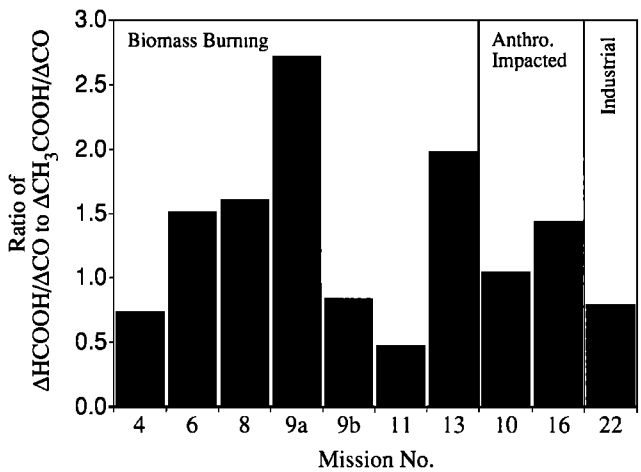

Fig. 9. Ratio of HCOOH and CH_3COOH in enhancement factors for each plume.

Combustion (biomass-burning and anthropogenic) appears to be the only known source of atmospheric $(COO^-)_2$. Only missions 10, 16, and 22 showed significant influence of anthropogenic pollution, as indicated by elevated C_2Cl_4 and F-12 mixing ratios. Samples from missions 16 and 22 demonstrated a strong correlation between CO and $(COOH)_2$, suggesting that urban/industrial combustion processes may be important sources for atmospheric oxalate. Although anthropogenic combustion appears to be a principal source of HNO_3 over parts of North America, biomass-burning seems to be a significant source of HNO_3 in the subarctic regions of Canada. Biomass-burning appears to be a primary source of HCOOH and CH_3COOH to the Canadian troposphere.

Future experiments should help determine if $(COO^-)_2$, HCOOH, and CH_3COOH are produced primarily from biomass-burning or urban/industrial combustion. Stable C isotopic analysis is one tool that could be used to help separate anthropogenic and biomass-burning derived $(COO^-)_2$, HCOOH, and CH_3COOH. More biomass-burning experiments, sampling fresh and aged emissions, might also shed some light on the processes which potentially produce HCOOH in biomass-burning plumes. In addition, HNO_3 should also be measured in these experiments to determine if it is directly emitted or not from natural and anthropogenic combustion.

Acknowledgments. We acknowledge the support of the staff of the NASA Wallops Flight Facility and the helpfulness and resourcefulness of the Electra crew. We thank the reviewers for their comments. The high-quality laboratory facilities at Canador College, North Bay, Ontario, are also greatly appreciated by the UNH group. In addition, we would like to thank all the GTE participants who assisted in transferring the many UNH shipping cases during the relocation of our field laboratory. This research was supported by the NASA Global Tropospheric Chemistry program and a NASA Graduate Student Researchers Program fellowship. This paper draws upon B. Lefer's thesis submitted in partial fulfillment of the Master of Science degree at the University of New Hampshire.

REFERENCES

Andreae, M. O., et al., Biomass-burning emissions and associated haze layers over Amazonia, *J. Geophys. Res.*, *93*, 1509-1527, 1988*a*.

Andreae, M. O., R. W. Talbot, T. W. Andreae, and R. C. Harriss, Formic and acetic acid over the central Amazon region, Brazil, 1, Dry season, *J. Geophys. Res.*, *93*, 1616-1624, 1988*b*.

Arnts, R. R., and B. Gay, Jr., Photochemistry of some naturally emitted hydrocarbons, final report, 600/3-79-081, U.S. Environ. Prot. Agency, Research Triangle Park, N. C., 1979.

Bakwin, P. S., et al., Reactive nitrogen oxides and ozone above a taiga woodland, *J. Geophys. Res.*, this issue.

Blake, D. R., D. F. Hurst, T. W. Smith Jr., W. J. Whipple, T.-Y. Chen, N. J. Blake, and F. S. Rowland, Nonmethane hydrocarbons in the

troposphere over central Canada, *J. Geophys. Res.*, 16,559-16,588, 1992.

Blake, D. R., T. W. Smith, T. Y. Cheng, W. J. Whipple, and F. S. Rowland, Effects of biomass-burning on summertime nonmethane hydrocarbon concentrations in the Canadian wetlands, *J. Geophys. Res.*, this issue.

Browell, E. V., M. A. Fenn, C. F. Butler, W. B. Grant, R. C. Harriss and M. C. Shipham, Ozone and aerosol distributions in the summertime troposphere over Canada, *J. Geophys. Res.*, this issue.

Cachier, H., H. Ducret, M.-P. Bremond, V. Yoboue, J.-P. Lacaux, A. Gaudichet, and J. Baudet, Biomass-burning aerosols in Savanna region of the Ivory Coast, in *Global Biomass-burning*, edited by J. S. Levine, pp. 174-180, MIT Press, Cambridge, Mass., 1991.

Cofer, W. R., III, V. G. Collins, and R. T. Talbot, Improved aqueous scrubber for collection of soluble atmospheric trace gases, *Environ. Sci. Technol.*, *19*, 557-560, 1985.

Cofer, W. R., III., J. S. Levine, P. J. Riggan, D. I. Sebacher, E. L. Winstead, E. F. Shaw Jr., J. A. Brass, and V. G. Ambrosia, Trace gas emissions from a midlatitude-prescribed chaparral fire, *J. Geophys. Res.*, *93*, 1653-1658, 1988.

Crutzen, P. J., and M. O. Andreae, Biomass-burning in the Tropics: Impact on atmospheric chemistry and biogeochemical cycles, *Science*, *250*, 1669-1677, 1990.

Crutzen, P. J., L. E. Heidt, J. P. Krasnec, W. H. Pollock, and W. Seiler, Biomass-burning as a source of atmospheric gases CO, H_2, N2O, CH_3Cl, and COS, *Nature*, *282*, 253-256, 1979.

Crutzen, P. J., A. C. Delany, J. Greenberg, P. Haagenson, L. Heidt, R. Leub, W. Pollack, W. Seiler, A. Wartburg, and P. Zimmerman, Tropospheric chemical composition measurements in Brazil during the dry season, *J. Atmos. Chem.*, *2*, 233-256, 1985.

Gorzelska, K., R. W. Talbot, K. Klemm, B. L. Lefer, O. Klemm, G. L. Gregory, B. Anderson, and L. A. Barrie, Chemical composition of the atmospheric aerosol in the troposphere over the Hudson Bay lowlands and Quebec-Labrador regions of Canada, *J. Geophys. Res.*, this issue.

Harriss, R. C., S. C. Wofsy, J. M. Hoell, Jr., R. J. Bendura, J. W. Drewry, R. J. McNeal, D. Pierce, V. Rabine, and R. L. Snell, The Arctic Boundary Layer Expedition (ABLE) 3B: July-August 1990, *J. Geophys. Res.*, this issue (*a*).

Harriss, R. C., G. W. Sachse, J. E. Collins, L. Wade, K. B. Bartlett, R. W. Talbot, E. V. Browell, L. A. Barrie, G. F. Hill, and L. G. Burney, Carbon monoxide and methane over Canada: July-August 1990, *J. Geophys. Res.*, this issue (*b*).

Hartmann, W. R., *Carbonsäuren in der Atmosphäre*, Ph.D. thesis, 106 p., Univ. of Mainz, Germany, 1990.

Helas, G., H. Bingemer, and M. O. Andreae, Organic acids over equatorial Africa: Results from DECAFE 88, *J. Geophys. Res.*, *97*, 6187-6193, 1992.

Howard, C. J., Rate constants for the gas-phase reactions of OH radicals with ethylene and halogenated ethylene compounds, *J. Chem. Phys.*, *65*, 4771-4777, 1976.

Jacob, D. J., and S. C. Wofsy, Photochemical production of carboxylic acids in a remote continental atmosphere, in *Acid Deposition Processes at High Elevation Sites*, edited by M. H. Unsworth, D. Reidel, Norwell, Mass, 73-92, 1988.

Jacob, D. J., et al., Summertime photochemistry of the troposphere at high northern latitudes, *J. Geophys. Res.*, *97*, 16,421-16,432, 1992.

Kawamura, K., and I. R. Kaplan, Biogenic and anthropogenic organic compounds in rain and snow samples collected in southern California, *Atmos. Environ.*, *20*, 115-124, 1986.

Keene, W. C., and J. N. Galloway, The biogeochemical cycling of formic and acetic acids through the troposphere: An overview of current understanding, *Tellus*, *40(B)*, 322-334, 1988.

Keene, W. C., and J. N. Galloway, Considerations regarding sources for formic and acetic acids in the troposphere, *J. Geophys. Res.*, *91*, 14,466-14,474, 1986.

Keene, W. C., J. N. Galloway, and J. D. Holden, Jr., Measurement of weak organic acidity in precipitation from remote areas of the world, *J. Geophys. Res.*, *88*, 5122-5130, 1983.

Keller, M., D. J. Jacob, S. C. Wofsy, and R. C. Harriss, Effects of tropical deforestation on global and regional atmospheric chemistry, *Clim. Change*, *19*, 139-158, 1991.

Klemm, O., and R. W. Talbot, A sensitive method for measuring atmospheric concentrations of sulfur dioxide, *J. Atmos. Chem.*, *13*, 325-342, 1991.

Lacaux, J.-P., R. A. Delmas, B. Cros, B. Lefeivre, and M. O. Andreae, Influence of biomass-burning emissions on precipitation chemistry in the equatorial forests of Africa, in *Global Biomass-burning*, edited by J. S. Levine, pp. 168-173, MIT Press, Cambridge, Mass., 1991.

LeBel, P. J., W. R. Cofer III, J. S. Levine, and S. A. Vay, Nitric acid and ammonia emissions from a mid-latitude prescribed wetlands fire, *Geophys. Res. Lett.*, *15*, 792-795, 1988.

Li, S.-M., and J. W. Winchester, Geochemistry of organic and inorganic ions of late winter Arctic aerosols, *Atmos. Environ.*, *23*, 2401-2415, 1989.

Logan, J. A., Nitrogen Oxides in the troposphere: Global and regional budgets, *J. Geophys. Res.*, *88*, 10,785-10,807, 1983.

Meyers, T. P., B. J. Huebert, and B. B. Hicks, HNO_3 deposition to a deciduous forest, *Boundary Layer Meteorol.*, *49*, 395-410, 1989.

Nojima, K., K. Fukaya, S. Fukui, and S. Kanno, The formation of glyoxals by the photochemical reaction of aromatic hydrocarbons in the presence of nitrogen monoxide, *Chemosphere*, *5*, 247-252, 1974.

Norton, R. B., J. M. Roberts, and B. J. Huebert, Tropospheric oxalate, *Geophys. Res. Lett.*, *10*, 517-520, 1983.

Sachse, G. W., G. F. Hill, L. O. Wade, and M. G. Perry, Fast-response, high-precision carbon monoxide sensor using a tunable diode laser technique, *J. Geophys. Res.*, *92*, 2071-2081, 1987.

Sandholm, S. T., et al., Summertime partitioning and budget of NO_y compounds in the troposphere over Alaska and Canada, *J. Geophys. Res.*, this issue.

Sanhueza, E., Effects of vegetation burning on the atmospheric chemistry of the Venezuelan Savanna, in *Global Biomass-burning*, edited by J. S. Levine, pp. 122-125, MIT Press, Cambridge, Mass., 1991.

Sanhueza, E., W. Elbert, A. Rondon, M. Corina Arias, and M. Hermoso, Organic and inorganic acids in rain from a remote site of the Venezuelan savannah, *Tellus*, *41(B)*, 170-176, 1989.

Shipham, M. C., A. S. Bachmeier, D. R. Cahoon, Jr., and E. V. Browell, Meteorological overview of the Arctic Boundary Layer Expedition (ABLE) 3A flight series, *J. Geophys. Res.*, 16,395-16,421, 1992.

Shipham, M. C., A. S. Bachmeier, D. R. Cahoon, Jr., G. L. Gregory, B. E. Anderson, and E. V. Browell, Meteorological interpretation of the Arctic Boundary Layer Expedition (ABLE) 3B flight series, *J. Geophys. Res.*, this issue.

Singh, H. B., et al., Summertime distribution of PAN and other reactive nitrogen species in the northern high-latitude atmosphere of eastern Canada, *J. Geophys. Res.*, this issue.

Talbot, R. W., M. O. Andreae, T. W. Andreae, and R. C. Harriss, Regional aerosol chemistry of the Amazon basin during the dry season, *J. Geophys. Res.*, *93*, 1499-1508, 1988*a*.

Talbot, R. W., K. M. Beecher, R. C. Harriss, and W. R. Cofer, Atmospheric geochemistry of formic and acetic acids at a midlatitude temperate site, *J. Geophys. Res.*, *93*, 1689-1698, 1988*b*.

Talbot, R. W., A. S. Vijgen, and R. C. Harriss, Measuring tropospheric HNO_3: Problems and prospects for nylon filter and mist chamber, *J. Geophys. Res.*, *95*, 7553-7542, 1990*a*.

Talbot, R. W., M. O. Andreae, H. Berresheim, D. J. Jacob, and K. M. Beecher, Sources and sinks of formic, acetic, and pyruvic acids over central Amazonia, 2, Wet season, *J. Geophys. Res.*, *95*, 16,799-16,811, 1990*b*.

Talbot, R. W., M. O. Andreae, H. Berresheim, P. Artaxo, M. Garstang, R. C. Harriss, K. M. Beecher, and S. M. Li, Aerosol chemistry during the wet season in central Amazonia: The influence of long-range transport, *J. Geophys. Res.*, *95*, 16,955-16,969, 1990*c*.

Talbot, R. W., A. S. Vijgen, and R. C. Harriss, Soluble species in the Arctic summer troposphere: Acidic gases, aerosols, and precipitation, *J. Geophys. Res.*, 16,531-16,545, 1992.

Talbot, R. W., et al., Summertime distribution and relations of reactive odd nitrogen species and NO_y in the troposphere over Canada, *J. Geophys. Res.*, this issue.

Wofsy, S. C., et al., Atmospheric chemistry in the Arctic and subarctic: Influence of natural fires, industrial emissions, and stratospheric inputs, *J. Geophys. Res.*, 16,731-16,746, 1992.

Wofsy, S. C., S.-M. Fan, D. R. Blake, J. D. Bradshaw, S. T. Sandholm, H. B. Singh, G. W. Sachse, and R. C. Harriss, Factors influencing atmospheric composition over subarctic North America during summer, *J. Geophys. Res.*, this issue.

J. D. Bradshaw, J. O. Olson, and S. T. Sandholm, School of Earth and Atmospheric Sciences, Georgia Institute of Technology, Atlanta, GA 30332.

K. Gorzelska, Now at Centralny Instytut Ochrony Pracy, Warsaw, Poland.

R. C. Harriss, B. L. Lefer, and R. W. Talbot, Institute for the Study of Earth, Oceans, and Space, University of New Hampshire, Durham, NH 03824.

K. I. Klemm and O. Klemm, Now at Fraunhofer-Institut fur Atmospharische Umweltforschung, Garmisch-Partenkirchen, Germany.

J. Barrick, J. Collins, G. W. Sachse, and M. A. Shipham, NASA Langley Research Center, Hampton, VA 23665.

D. R. Blake, Department of Chemistry, University of California-Irvine, Irvine, CA 92717.

(Received February 1, 1993;
revised July 19, 1993;
accepted July 27, 1993.)